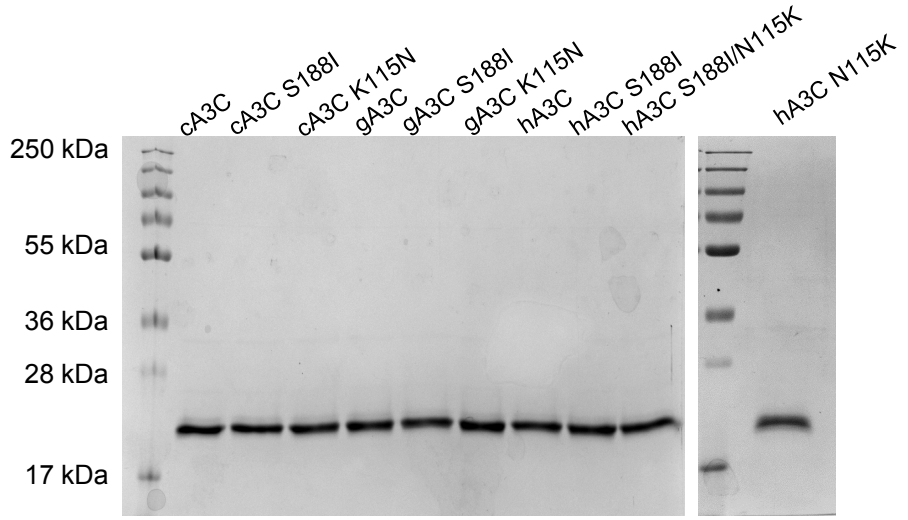

Figure S1. SDS-PAGE of purified A3C enzymes. GST-tagged A3C enzymes were affinity purified with glutathione sepharose, the GST tagged was cleaved with thrombin, and the A3C was purified from the free GST and thrombin using a DEAE column (GE Healthcare).

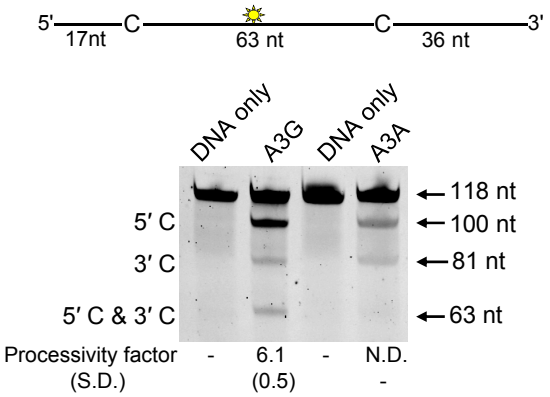

Figure S2. Processivity of A3G and A3A. Processivity of A3 enzymes was tested on an ssDNA substrate that contained fluorescein-labeled deoxythymidine (yellow star) between two 5′CCC (A3G) or 5′TTC (A3A) deamination motifs. Deamination of a 118 nt ssDNA substrate with deamination targets spaced 63 nt apart. Single deaminations of the 5′ C & 3′ C are detected as the appearance of labeled 100- and 81- nt fragments, respectively; double deamination of both C residues on the same molecule results in a 63 nt labeled fragment. A measurement using the integrated gel band intensities determines a processivity factor that indicates the likelihood of the enzyme to deaminate both motifs in a single enzyme-substrate encounter (see Materials & Methods). If no 5′C & 3′C band was detected, the processivity was denoted with N.D. (not detected) and means that the enzyme is not processive. The measurements of enzyme processivity (processivity factor) and the S.D. are shown below the gels. All values are calculated from at least three independent experiments.

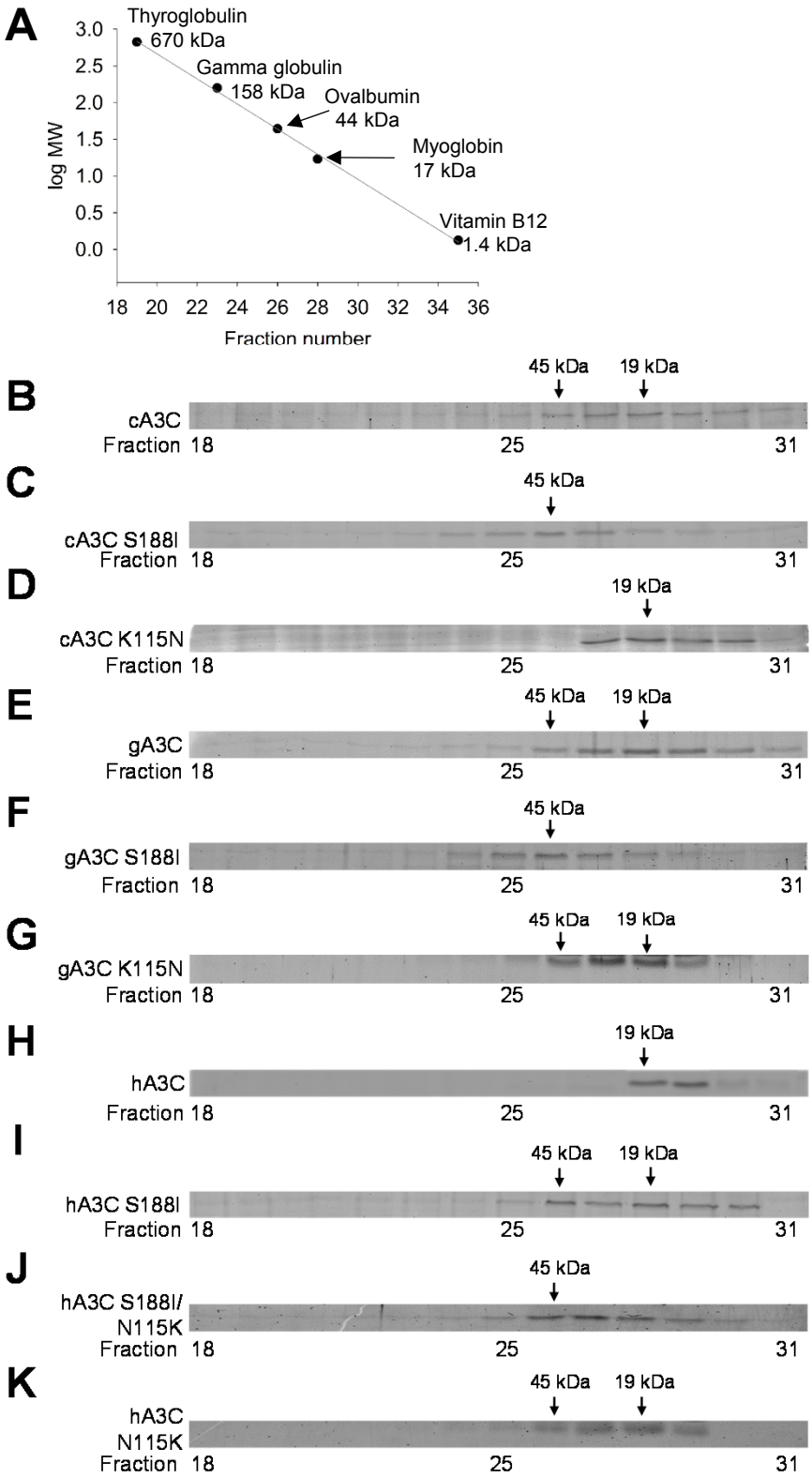

Figure S3. SDS-PAGE of size exclusion chromatography resolved fractions of A3C enzymes. (A) The standard curve obtained from the 10 ml Superdex 200 column from which molecular weight and oligomerization states where calculated (see Figure 3). (B-K) The chromatograms from the 10 ml Superdex 200 column were constructed by analyzing the integrated gel band intensities of the protein in each fraction after resolution by SDS-PAGE (see Figure 3). The gels for each panel were resolved, stained with Oriole stain, and scanned in parallel. The gels show the size exclusion chromatography fractions resolved by SDS-PAGE for each A3C, as labeled on each panel. The molecular weight calculated from the standard curve are shown for the peak fractions.

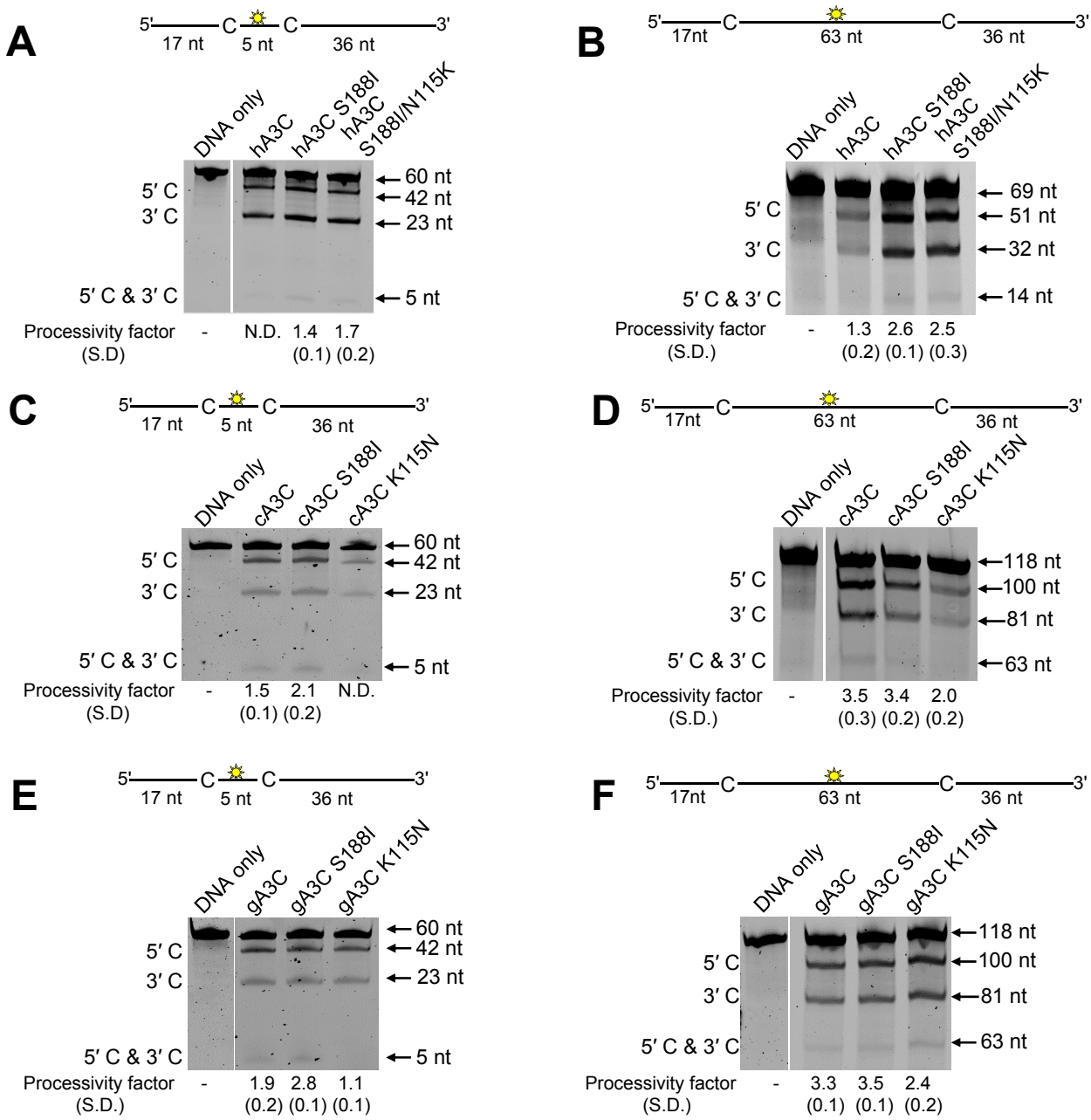

Figure S4. Analysis of A3C wild type and mutant processive ssDNA scanning. Processivity of A3C enzymes was tested on ssDNA substrates that contained fluorescein-labeled deoxythymidine (yellow star) between two 5′TTC deamination motifs. Deamination targets were separated by 5- or 63- nt. (A, C, E) Deamination of a 60 nt ssDNA substrate with deamination targets spaced 5 nt apart for (A) hA3C, (C) cA3C, and (E) gA3C. Single deaminations of the 5′ C & 3′ C are detected as the appearance of labeled 42 and 23 nt fragments, respectively; double deamination of both C residues on the same molecule results in a 5 nt labeled fragment. (B, D, F) Deamination of a 118 nt ssDNA substrate with deamination targets spaced 63 nt apart for (B) hA3C, (D) cA3C, and (F) gA3C. Single deaminations of the 5′ C & 3′ C are detected as the appearance of labeled 100 and 81 nt fragments, respectively; double deamination of both C residues on the same molecule results in a 63 nt labeled fragment. If no 5′C & 3′C band was detected, the processivity was denoted with N.D. (not detected). Samples for each panel were resolved on the same gel. A white line means that lanes in between the lanes shown were removed for clarity of presentation. The measurements of enzyme processivity (processivity factor) and the S.D. are shown below the gels. All values are calculated from at least three independent experiments.

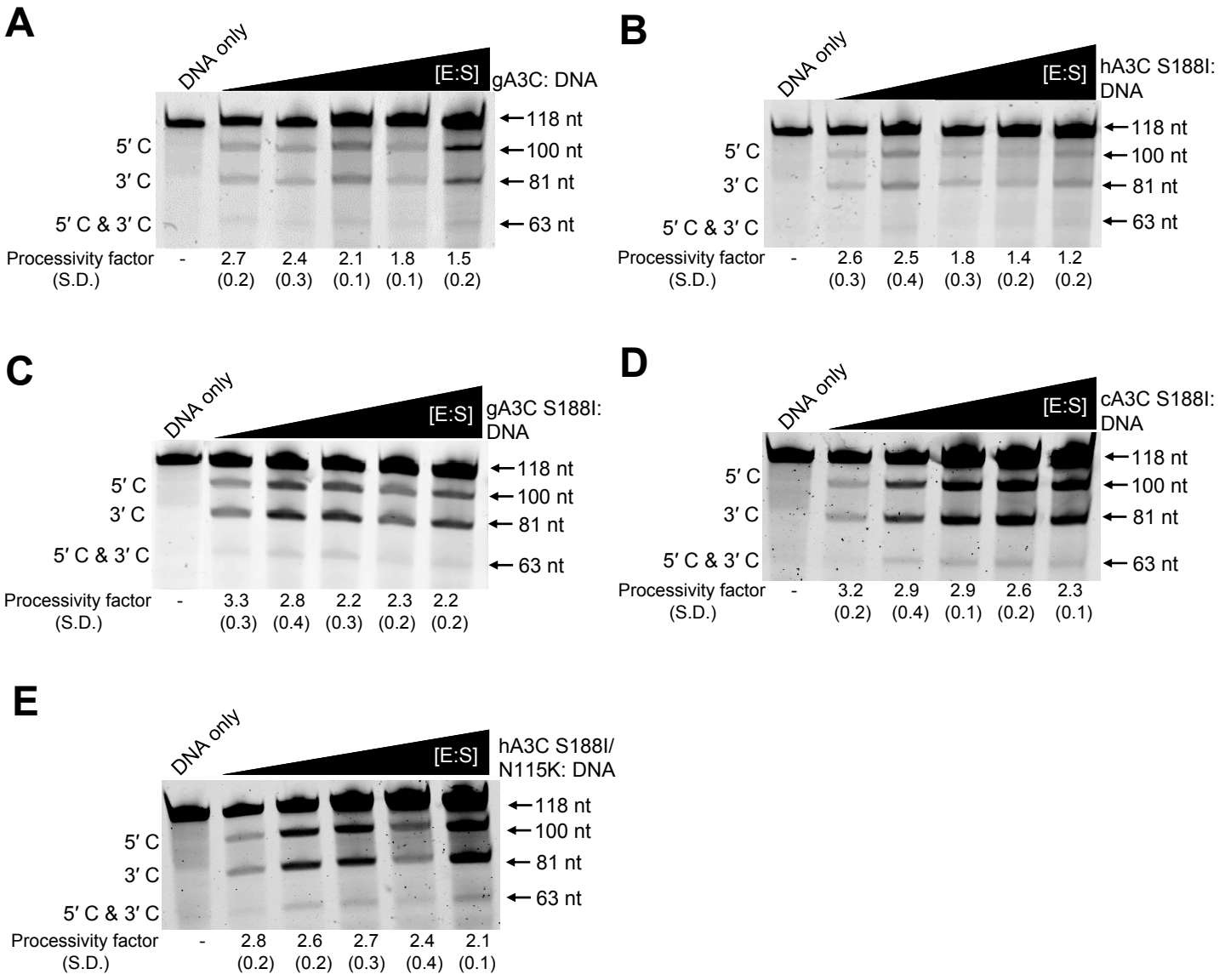

Figure S5. Intersegmental transfer ability of A3C is determined by the oligomeric state. The ssDNA substrate contained a fluorescein-labeled deoxythymidine (yellow star) between two 5′TTC deamination motifs. The deamination targets were separated by 63 nt. Intersegmental transfer ability of (A) gA3C (monomer/dimer), (B) hA3C S188I (monomer/dimer), (C) gA3C S188I (dimer), (D) cA3C S188I (dimer), and (E) hA3C S188I/N115K (dimer) was determined by keeping an A3C/ssDNA ratio of 3:1 constant, but increasing the total reaction components. If the enzyme is able to undergo intersegmental transfer, the assay will result in an apparent decrease in the processivity factor with increasing concentrations of reaction components. The measurements of enzyme processivity (processivity factor) and the S.D. are shown below the gels. All values are calculated from at least three independent experiments.

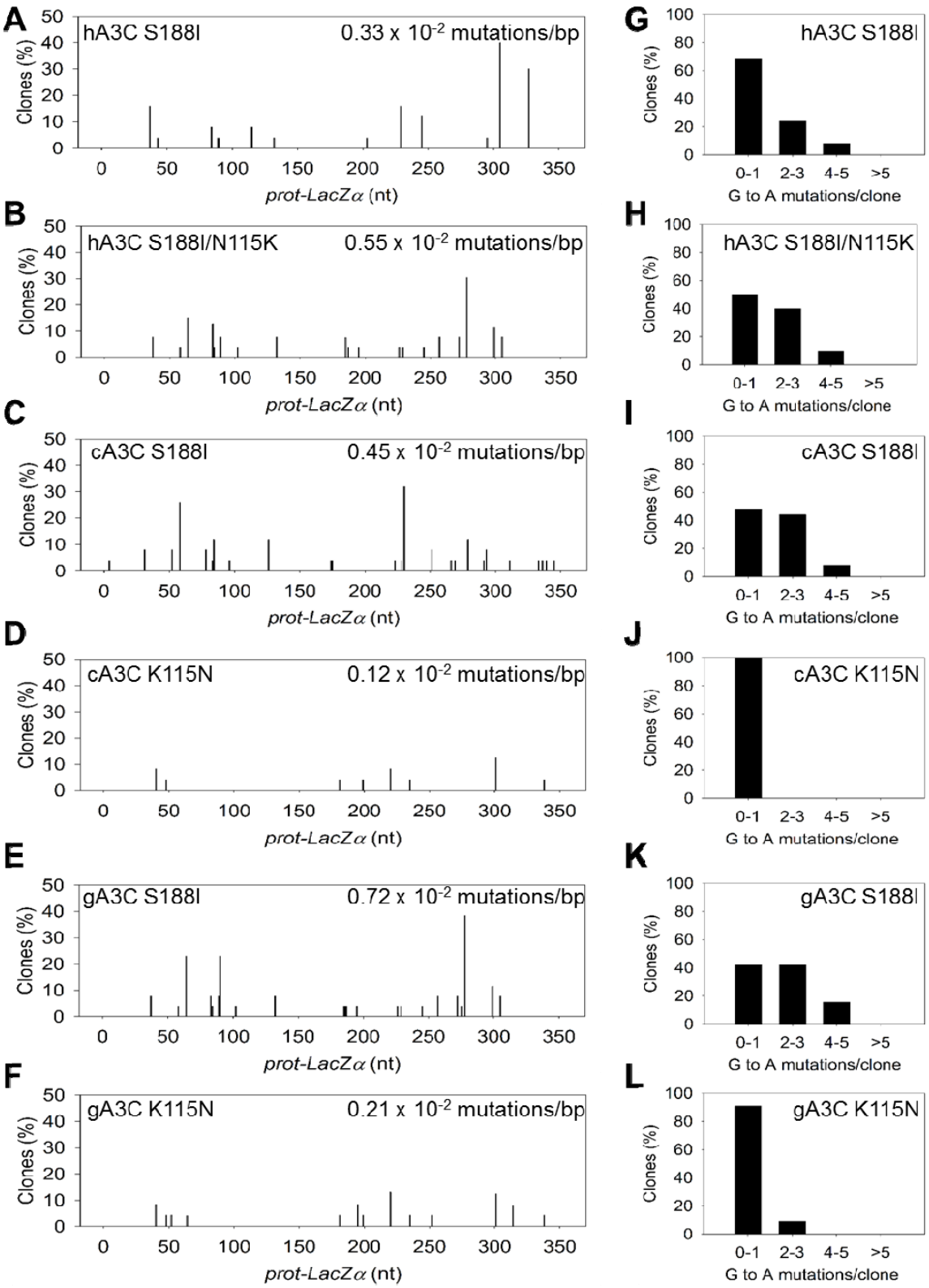

Figure S6. **Ability to dimerize correlates with increased mutagenesis *in vitro.*** An *in vitro* HIV reverse transcription assay was utilized to determine the mutant A3C enzymes abilities to catalyze deaminations during proviral DNA synthesis. (A–F) Spectra of mutations are plotted as the percentage of clones containing a mutation at a particular location (nt) in the 368 nt *prot-lacZα* construct for (A) hA3C S188I, (B) hA3C S188I/N115K, (C) cA3C S188I, (D) cA3C K115N, (E) gA3C S188I, (F) gA3C K115N. (G-L) Histograms illustrate the number of mutations per clone that can be induced by (G) hA3C S188I, (H) hA3C S188I/N115K, (I) cA3C S188I, (J) cA3C K115N, (K) gA3C S188I, (L) gA3C K115N.

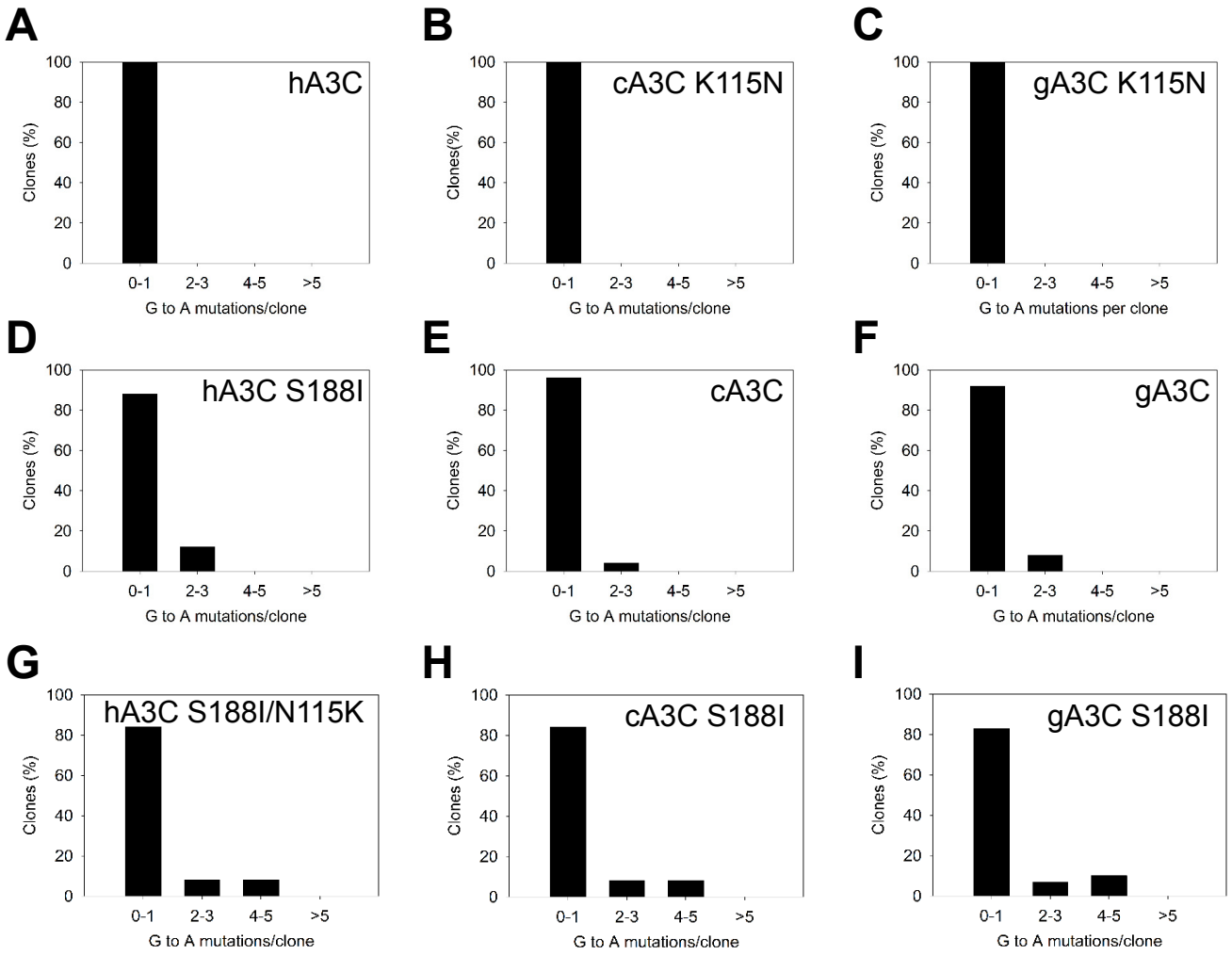

Figure S7. **Ability to dimerize correlates with increased mutagenesis in integrated proviral HIV Δvif DNA.** A single-cycle infectivity assay was utilized to determine the ability of A3C enzymes to catalyze deaminations during proviral DNA synthesis. Histograms illustrate the number of mutations per integrated proviral DNA clone that can be induced by (A) hA3C, (B) cA3C K115N, (C) gA3C K115N, (D) hA3C S188I, (E) cA3C (F) gA3C, (G) hA3C S188I/N115K, (H) cA3C S188I, and (I) gA3C S188I.